Peer-reviewed version available at *Water* **2020**, *12*, 364; doi:10.3390/w12020364

Article

High-Resolution Integrated Hydrological Modeling of Climate Change Impacts on a Semi-arid Urban Watershed in Niamey, Niger

Abdou Boko Boubacar[1, 2], Konaté Moussa[2], Nicaise Yalo[3], Steven J. Berg[4,5], Andre R. Erler[4,6], Pibgnina Bazié[7], Hyoun-Tae Hwang[5,6], Ousmane Seidou[8], Albachir Seydou Niandou[9], Keith Schimmel[9,*] and Edward A. Sudicky[5,6]

1 Graduate Research Program on Climate Change and Water Resources, West African Science Service Centre on Climate Change and Adapted Land Use (WASCAL), Université D'Abomey Calavi, Cotonou 03 BP 526, Benin; abdouboko@gmail.com
2 Département de Géologie, Faculté des Sciences et Techniques, Université Abdou Moumouni de Niamey, BP: 10 662; konate.moussa@gmail.com
3 University of Abomey Calavi, National Water Institute, Cotonou 03 BP 526, Benin; yalonicaise@yahoo.fr
4 Aquanty Inc., 564 Weber Street North, Waterloo, ON, Canada; sberg@aquanty.com
5 Department of Earth and Environmental Sciences, University of Waterloo, ON, Canada; hthwang@aquanty.com, esudicky@aquanty.com, hthwang@aquanty.com
6 Department of Physics, University of Toronto, ON, Canada; AErler@aquanty.com
7 AGRHYMET Regional Center, Niamey, Niger; p.bazie@agrhymet.ne
8 Department of Civil Engineering, University of Ottawa, ON, Canada; Ousmane.Seidou@uottawa.ca
9 Applied Science and Technology, North Carolina Agricultural and Technical State University, Greensboro, NC 27411, USA; albachir@sahelconsulting.com
* Correspondence: schimmel@ncat.edu

Abstract: This study evaluated the impact of climate change on water resources in a large semi-arid urban watershed located in Niamey Republic of Niger, West Africa. The watershed was modeled using the fully integrated surface-subsurface HydroGeoSpheremodel at a high spatial resolution. Historical (1980-2005) and projected (2020-2050) climate scenario derived from the outputs of three Regional Climate Models (RCM) under the RCP 4.5 scenario were statistically downscaled using the multiscale quantile mapping bias correction method. Results show that the bias correction method is optimum at daily and monthly scales, and increased RCM resolution does not improve the performance of the model. The three RCMs predict increases of up to 1.6% in annual rainfall and of 1.58°C for mean annual temperatures between the historical and projected periods. The durations of the Minimum Environmental Flow (MEF) conditions, required to supply drinking and agriculture water, were found to be sensitive to changes in runoff resulting from climate change. MEF occurrences and durations are likely to be greater for (2020-2030), and then they will be reduced for (2030-2050). All three RCMs consistently project a rise in groundwater table of more than 10 meters in topographically high zones where the groundwater table is deep and an increase of 2 meters in the shallow groundwater table.

Keywords: climate change; integrated hydrological model; semi-arid; impacts

1. Introduction

The Niger River is the primary surface water used for agriculture and drinking water supply for Niamey, Niger, West Africa (located in the middle Niger River basin, see Figures 1a and 1b). Given that the water distribution network does not cover the entire populated area and because of recurrent droughts, the Niger River cannot provide the total water demand for the area. Groundwater is pumped through open wells and boreholes to provide water to more than 35% [1] of the 1.3 million

[2] city population. The share of groundwater in the water supply for drinking and agriculture purposes is increasing due to rapid population growth and urbanization. Simultaneously, episodes of extreme low flows have become more frequent because of a combination of increasing demand, sedimentation of the riverbed, and increased variability in streamflow upstream of Niamey. Therefore, the minimum environmental flow for Niamey, set to 55 m^3/s over 10 days, is often violated. Authorities in Niger fear groundwater resources may become insufficient and/or the violations of the minimum environmental flow will become more severe and more frequent in the future as a result of climate change and increased demand. Therefore, a study that will investigate the behavior of the whole hydrological system in the area under climate change is important.

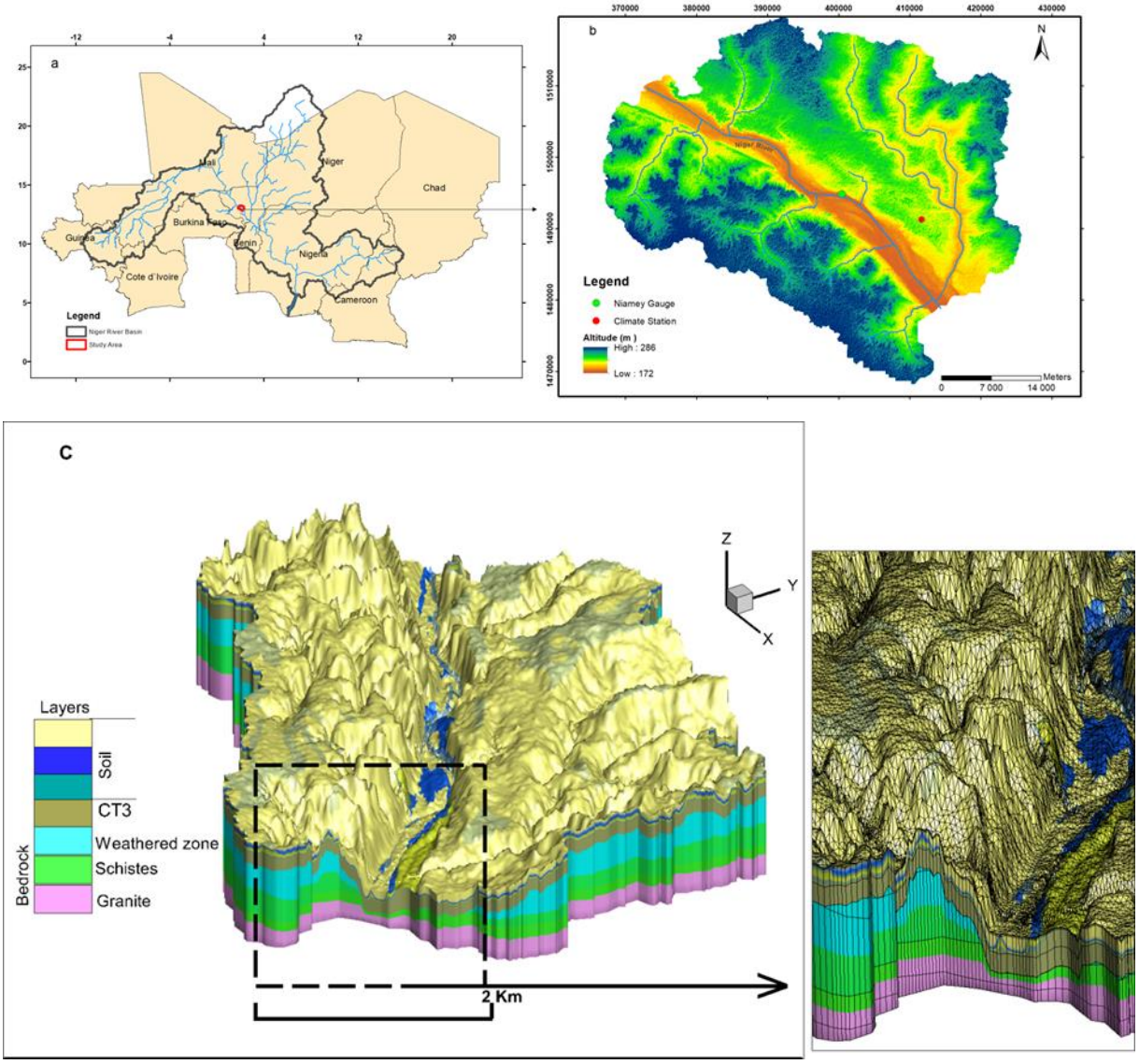

Figure 1. (a) Study area location within the Niger River basin; (b) Local context of the study area with topography and streams network; (c) 3D surface-subsurface model of the study area.

Understanding the impacts of climate change and hydrological extremes on water resources remains a central issue for sustainable water resources management. The impacts are likely to alter the hydrological cycle and induce negative effects on the availability and quality of water resources [3]. Changes in temperature and precipitation, combined with changes in the frequency and intensity of extreme hydro-meteorological events, will most likely have important implications for water resources by affecting the supply, quality, and distribution of water for billions of people [4]. However, the effects of climate change are not expected be distributed evenly between sectors,

regions, communities, households, and individuals. Some are likely to be particularly vulnerable to changes in the global water system.

Even though the simulation of the impact of climate change on water resources is highly uncertain [5-14], there is a high confidence African water resources systems are among the most vulnerable to climate change [15]. Uncertainties are particularly high when it comes to groundwater resources [16]. Most studies [16-21] have been focused on climate change impacts on surface water, often neglecting groundwater, which is more complicated to model and assumed to be less vulnerable to climate change. Moreover, few [22-24] have considered large-scale, fully-integrated hydrological models when investigating climate change impacts.

While most arid regions rely on groundwater for agriculture and drinking water supplies [25], little attention has been given to climate change impacts on groundwater in Africa [16,17,26,27]. Most studies use saturated groundwater flow models or loosely coupled surface water-groundwater models to investigate climate change impacts on groundwater. Major issues in these studies include the estimation of aquifer recharge and the use of over simplistic bias-correction methods for projected climate time series.

Aquifer recharge is the most important parameter in the hydrological cycle, connecting directly groundwater to the atmosphere, and any error in its estimate leads to significant variability in the projected change in groundwater reserves. The groundwater recharge process in arid environments is mainly driven by localized recharge through surface water features [28-31], which is not adequately represented in saturated groundwater flow models, where groundwater recharge is a user specified parameter. In these models, there is a linear relationship between groundwater recharge and evapotranspiration derived from climate forcing data.

It has been shown that biases are significant in most climate change impact studies on water resources [32]. These biases often determine the direction of climate change impacts on water resources. Therefore, a better estimation of evapotranspiration may lead to a better estimation of climate change impacts on water resources. This may be achieved through the use of fully-integrated models capable of calculating actual evapotranspiration and able to integrate different recharge processes (focused recharge, direct recharge, GW-SW) considering land-use types [22-24,33]. In fully integrated hydrological models, groundwater recharge is no longer user-specified but part of the solution provided by the model. There is no systematic linear relationship between groundwater recharge and climate forcing data, and evapotranspiration is computed internally and spatially, considering different land use, surface water features, and subsurface hydrostratigraphy.

This paper uses state-of-the-art high resolution, fully-integrated hydrological models and multiscale statistical bias correction to investigate climate change impacts on groundwater resources in the Niger River basin. The objectives of the paper are to evaluate: (1) the potential climate change impacts on groundwater resources, and (2) the frequency and duration of the minimum environmental flows for the next thirty years using state-of-the-art hydrological models and multiscale statistically downscaled RCMs.

2. Materials and Methods

2.1 Study area

The study area is a 1,900 km² subwatershed of the middle Niger River basin (Figure 1a) and is located southwest of the Republic of Niger. The Niger River is used to provide water for agricultural purposes and to meet the drinking water needs of 65% of the 1.3 million people in Niamey [1]. The remaining 35% is supplied by groundwater from two different aquifers: (1) the fractured aquifers of the Liptako basement, and (2) the sedimentary aquifer of the Continental terminal 3 (Figure 1c). The water bearing formations of the fractured aquifer are Paleoproterozoic in age (2300-2000 Ma) [34] and are composed of granitoid plutons alternating with greenstone belts. The greenstone belts are composed of metamorphosed sandstones-pelitic rocks (shales, sericite schists, micaceous schists, quartzitic schists) and low to medium metamorphic greenstone (amphibolite, chloritoschists, metabasalts, metagabbros) [34-36]. The Continental Terminal aquifer is mainly composed of clayish

to silty sandstones interbedded with oolithes and clay lenses and overlays a major unconformity with the Liptako basement formation.

The topographic high within the study area corresponds to the CT3 plateau with elevations ranging from 190 m to 250 m (a.s.l.), while the low land area is occupied by plains containing ephemeral streams and ponds with elevations ranging from between 178 m to 185 m (Figure 1b). Ephemeral streams act as temporary tributaries of the Niger River and are depression focused groundwater recharge areas [37]. Runoff collected by the ephemeral stream is generally discharged into several temporary and or permanent ponds that are located in the course of the ephemeral streams. The ponds act as groundwater recharge/discharge areas during the rainy/dry season [37].

Climate in the area is semi-arid and characterized by low frequency intense rainfall events occurring from June to September (rainy season). There is no rainfall in the long dry season spanning from October to May (Figure 2). The mean annual rainfall for 1980-2009 is estimated as 514 mm with a standard deviation of 116 mm [38], highlighting the important temporal rainfall interannual variability. The average temperature in the study area is 29°C, while evapotranspiration is 2,500 mm per year [39].

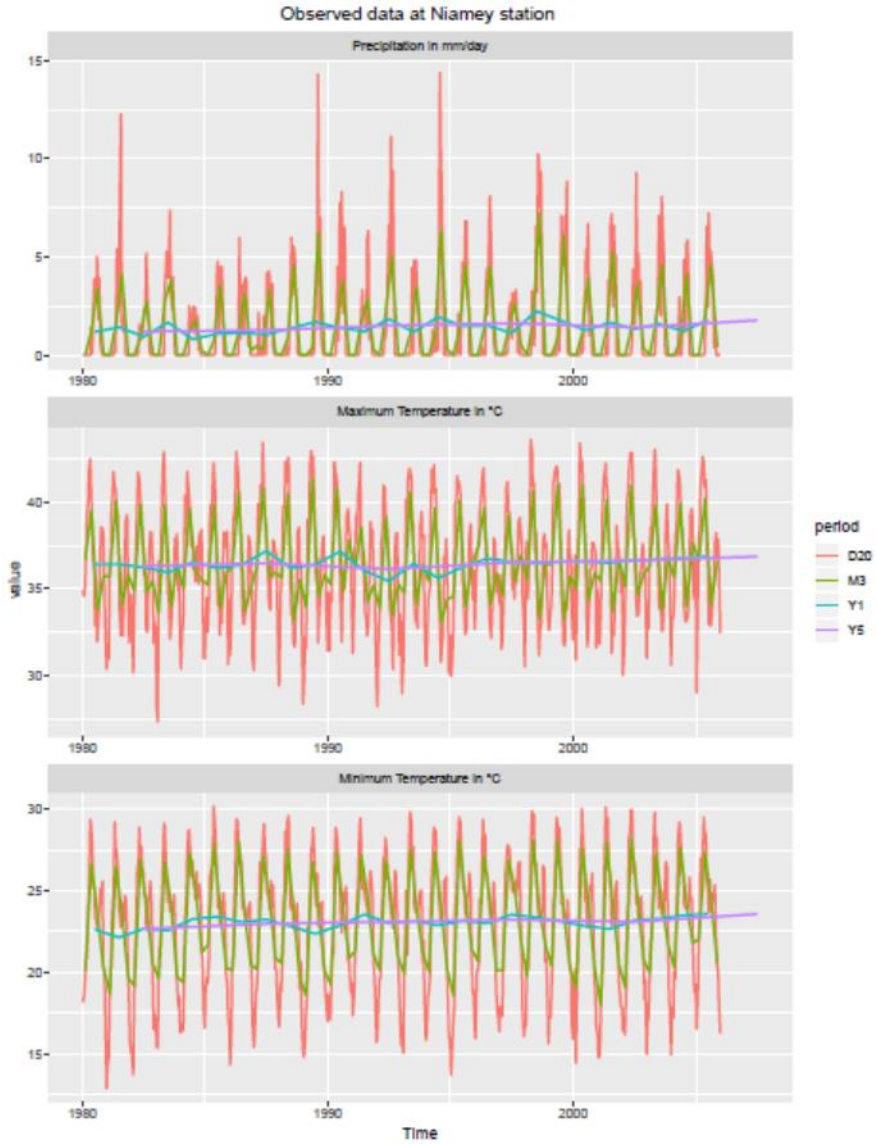

Figure 2. Observed rainfall, maximum temperatures, and minimum temperatures for 1980-2005 at Niamey Airport.

2.2 Integrated hydrological model

2.2.1 Mathematical and numerical model

The hydrological model used to simulate climate change impact over the study area is the fully distributed, tightly-coupled, surface-subsurface, three-dimensional, finite element model HydroGeoSphere (HGS) [40]. The 3D modified form of the Richards' equation in the variably saturated subsurface flow domain and the 2D depth-integrated diffusion wave equation for surface water flow are simultaneously solved in HGS in a parallelized manner [41].

One important source of uncertainty in climate change impacts simulation is the calculation of evapotranspiration, a key connector between climate projections and the hydrological model [32,42]. The biases in evapotranspiration estimates can be reduced by describing it as a mechanistic process [32]. While evapotranspiration is a user-defined input in most studies, the evapotranspiration model used in HGS is a mechanistic process driven by the potential evapotranspiration controlled by transpiration parameters, soil moisture, land-use type, leaf area index (LAI) and rooting depth [43]. Such a representation allows the reduction of biases in evapotranspiration biases using a mechanistic evapotranspiration model as is done in climate models. Thus, the evapotranspiration model can be simplified based on the purposes of studies [44,45].

The evapotranspiration model used in this study is based on [43] and assumes that evaporation and transpiration affects both the surface and subsurface flow systems, when evaporation is a result of the energy penetrating the vegetation cover. Detailed information on the evapotranspiration implemented in HGS can be found in the HGS documentation [40]. The transpiration rate ($\boldsymbol{T_p}$) is calculated using a function of a set of parameters that describe the net capacity of transpiration:

$$\boldsymbol{T_p = f_1(LAI)\, f_2(\theta)\, RDF\, (E_p - E_{can})} \quad (1)$$

where $\boldsymbol{f_1(LAI)}$ is a function of leaf area index, $\boldsymbol{f_2(\theta)}$ is a function of nodal water content, and RDF is the time-varying root distribution function. The surface and subsurface evaporation can be expressed as:

$$\boldsymbol{E_s = \alpha^*\left(E_p - E_{can}\right)\left[1 - f_1(LAI)\right] EDF} \quad (2)$$

where $\boldsymbol{\alpha^*}$is the wetness factor based on surface water depths and subsurface soil saturations and *EDF* is the evaporation distribution function that includes the surface/subsurface flow domains.

2.2.2 Discretization and calibration

The 1,900 km^2 area of the basin was discretized into triangular mesh elements with a total of 516,901 nodes and 927,030 elements. The horizontal resolution of the 2D mesh elements ranged from 70 m at the vicinity of surface water features to 350 m in the rest of the model domain. The HGS model was sequentially calibrated with increasing temporal resolution at steady state, dynamic equilibrium, and fully transient conditions as described in [37]. The outer subsurface model domain boundaries were assumed to correspond to groundwater flow divides, and no-flow boundary conditions were assigned. Precipitation and PET were assigned to the top of the model as hydroclimate forcing variables. A critical depth condition was prescribed to the outer edge boundary of the model at the outlet of the watershed to let surface water flow out of the model domain. To represent the surface water flowrate generated upstream (outside) of the study area, a surface water flux boundary condition was assigned at the most northern point. The discretization and calibration of the model as well as the boundary conditions are described in more details in [37].

2.3. Hydroclimatic data

2.3.1 Historical climate data

The model was forced with daily transient data of twenty-five years (1980-2005) observed precipitation along with maximum and minimum temperature (Tmax, Tmin) data from the Niamey Airport station (Figure 2). Potential evapotranspiration was calculated using the Hargreaves method:

$$ET_o = 0.0023 \times 0.408\, RA \times (T_{avg} + 17.8) \times TD^{0.5} \quad (3)$$

where $\mathbf{ET_o}$ is the reference evapotranspiration, RA is extraterrestrial radiation expressed in MJ m^{-2} d^{-1}), $\mathbf{T_{avg}}$ is the average daily temperature (°C) defined as the average of the mean daily maximum and mean daily minimum temperatures, TD is the temperature range estimated as the difference between mean daily maximum and mean daily minimum temperatures, and $\mathbf{0.408}$ corresponds to the constant used to convert the radiation to evaporation equivalents in mm. Hargreaves reference evapotranspiration method is recommended when there is not sufficient data to compute the Penman Montheith reference evapotranspiration [46].

2.3.2 Hydrological data

The Niamey gauging station was used to calibrate the model for surface water flow using twenty-five years (1980-2005) of daily stream flow data provided by the Niger Basin Authority (NBA). Twenty-five groundwater observations wells were used for steady-state groundwater heads calibration for 1980-2005. No transient groundwater head observation data are available for the 1980-2005 simulation period, and the model was previously calibrated for 2012-2017 with transient data [37]. While uncertainty related to groundwater models may be important between calibration and prediction periods, these uncertainties are considerably reduced for physically-based models even with different climatic conditions between calibration and prediction periods [10]. Therefore, the physically-based HGS's simulated groundwater heads for 1980-2005 could be used to predict climate change impacts on groundwater based on the HGS calibrated simulation of 2012-2017 in the absence of observations with relatively less uncertainties.

2.3.3 Climate projections

The outputs of two regional climates models of the CORDEX experiment at 50 km resolution and one high-resolution Regional Climate Model (RCM) of the West African Science Service Center on Climate Change and adapted land use (WASCAL) experiment at 12 km resolution were selected as climate projections. Only RCP (Representative Concentration Pathway) 4.5 was used because of the limited computational resources available and the fact that the differences between RCP 4.5 and RCP 8.5 are minimal before 2040 [47]. CANRCM4-CANESM2 and RCA4-IPSL-CM5A are the two RCMs selected from the CORDEX experiment based and on their ability to reproduce the hydrological cycle in the Niger River basin [48]. The metrics used to evaluate the models are well described in [48]. The WASCAL WRF-GFDELM-ESM2M at 12 km resolution was selected to evaluate the added value of the high resolution. Table 1 describes the configuration of the RCMs runs, including forcing Global Climate Models (GCMs) and RCM resolutions.

Table 1. RCMs and the forcing GCMs used in this study.

Institution	RCM	GCM	Resolution
Canadian Centre for Climate Modelling and Analysis	CanRCM4	CanESM2	50 km
Institut Pierre-Simon Laplace, France	RCA4	IPSL -CM5A	50 km
West African Science Service Center on Climate Change and Adapted Land Use (WASCAL)	WRFV3.5.1	GFDL-ESM2M	12 km

2.3.4 Bias correction

Hydrological impacts of climate change are typically evaluated using dynamical or statistical bias corrected climate output as forcing to the hydrological models. Dynamical downscaling involves the use of physics-based, RCMs with relatively higher resolution than the forcing GCM. Theoretically, the higher resolution allows a direct resolution of relevant local climate features. Dynamic downscaling is computationally expensive, and its use in large-scale hydrological impact studies is hence limited. It is much easier to use statistical bias correction methods, which generate a mapping function between predictor fields derived from observed local climate to local climate variables. The mapping function converts the simulated climate outputs into corrected time series whose statistical properties are closer to that of the local observed climate data. The calibration of the mapping function is usually done for the historical or control period, where observed data are available. The calibrated mapping function is then applied on the prediction period to obtain climate change projections.

However, commonly used statistical bias correction methods in hydrological climate impact studies assumes the mapping function to be valid at all temporal resolutions. Thus, it may introduce errors in impacts studies [49] and introduce a multiscale bias correction to allow different mapping functions at different scales. The method uses a standard quantile mapping method iteratively at multiple combined timescales (daily, monthly, and annual). To reduce potential errors associated with the stationary assumption, historical and projected climate output from the three RCMs were bias corrected to the observed climate station at Niamey Airport using two different methods: (1) standard quantile mapping calibrated at daily timescale, and (2) multiscale bias correction calibrated at daily (D1), monthly (M1), seasonal (M3), and annual (Y1) timescales. A comparison between the two methods was then performed to choose the best bias correction method. Statistical downscaling was applied to historical (1980-2005) and mid-century (2020-2050) periods for each climate model, resulting in a total of six (25 and 30 years) daily transient simulations.

3. Results and discussion

In this section, the biases of uncorrected and corrected RCM simulations of precipitation and evapotranspiration are examined and simulated groundwater heads and depth to groundwater as simulated by the HGS model are compared to observations. The projections of the HGS model in terms of groundwater recharge and minimum environmental flows are presented and discussed.

3.1 Biases in uncorrected and corrected historical climate simulations

The observed historical (1980-2005) rainfall and temperatures data at Niamey airport station (Figure 2) are compared at different timescales in Figure 3 with the basin weighted average uncorrected historical precipitation simulated by the three RCMs models. Rainfall biases are plotted as relative differences between historical observed and simulated data, while biases in temperatures are calculated as absolute differences averaged over different season. DJF is the December-January-February season; JJA corresponds to June-July-August and is the rainy season; MAM and SON are respectively March-April-May and September-October-November periods (Figure 3).

Considerable differences in the statistical characteristics of the mean biases at different timescales can be seen in Figure 3. The biases increase when time interval increase from daily to monthly, sub-seasonal, and seasonal (yearly) averages with increasing levels of biases. CANRCM4 and WRF present the largest biases in mean precipitation, while the RCA4 has less bias in rainfall and temperatures data. All the three regional models perform better during the JJA period, which corresponds to the rainy season, confirming the ability of the selected models to reproduce the precipitation seasonal cycle [47,48]. All three RCMs have large positive biases in mean simulated historical rainfall compared to observed historical rainfall. Rainfall biases are greater for the CANRCM4 model, followed by the WRF and RCA4 models, particularly for the MAM period, where

Preprints (www.preprints.org) | NOT PEER-REVIEWED | Posted: 25 December 2019 doi:10.20944/preprints201912.0329.v1

Peer-reviewed version available at Water 2020, 12, 364; doi:10.3390/w12020364

the biases in mean reached up to 300%. The observed large biases are probably due to the general wet days biases of uncorrected RCMs.

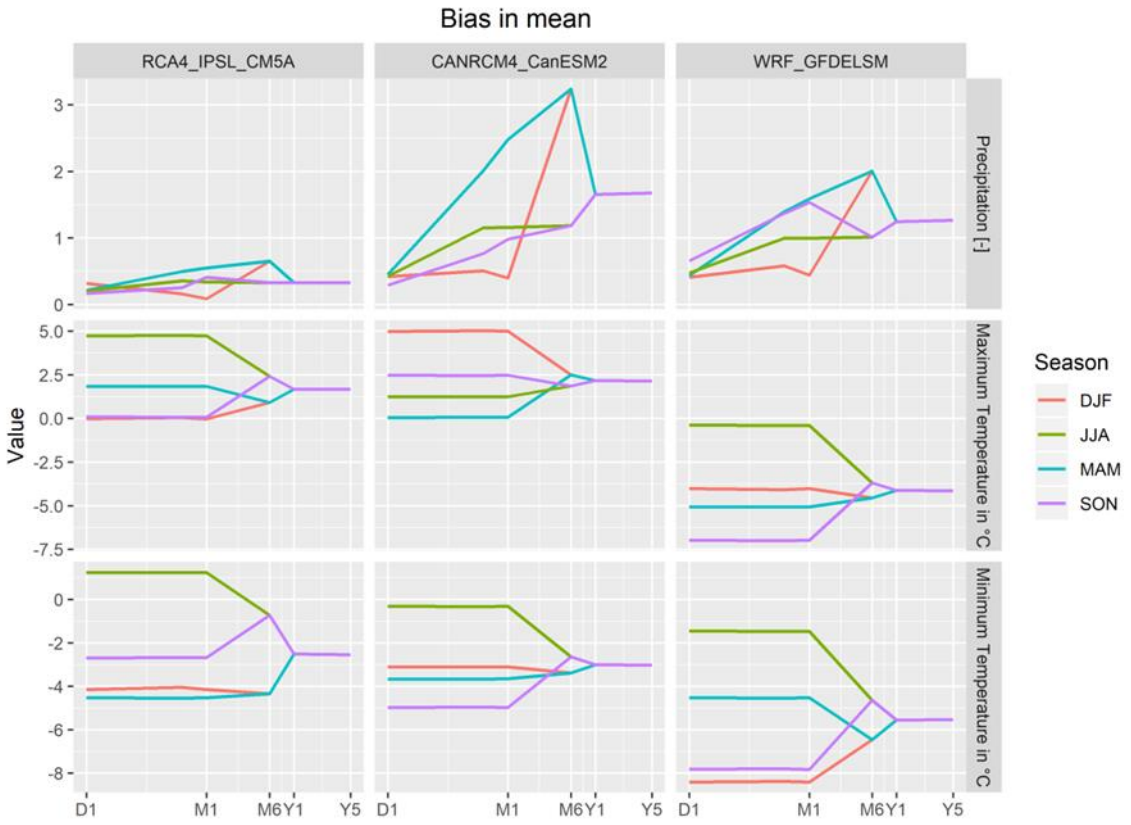

Figure 3. Bias in mean basin-average precipitation and temperature at different timescales between observed and simulated climate model data for the historical period (1980-2005).

As for the temperatures, the CANRCM4 and RCA4 models show positive maximum temperatures biases, whereas the WRF model is negatively biased for all seasons. The three RCMs have negative minimum temperatures biases for all the seasons except for the JJA period, where they are positively biased with the WRF recording the largest minimum temperature biases. Biases calculated using corrected and original (uncorrected) rainfall along with maximum and minimum temperatures time series for the three RCMs are shown in Figures 4a, 4b and 4c for the standard and multiscale quantile-quantile mapping bias correction methods and for different seasons of the year. The observed historical climate data (see Figure 2) is used to evaluate the performance of the two bias correction methods for the three RCMs for the simulated historical period (1980-2005). In Figures 4a, 4b, and 4c, residual biases are averaged and expressed as relative differences values (to observed historical) for rainfall data and in absolute differences for temperatures data at daily (D1), monthly (M1), and yearly (Y1) timescales.

The bias in rainfall calculated with the uncorrected WRF historical data (Figure 4a) vary from 50% to more than 250% across different periods with large biases recorded for the SON period. Simulated rainfall data for the RCA4 model are relatively less biased with the MAM period recording the largest bias of about 100% (Figure 4b). The CANRCM4 model has relative rainfall biases ranging from less than 100% to more than 450% with the MAM period having the largest bias (Figure 4c). The mean rainfall biases increase from daily to monthly temporal scale, then decrease at yearly timescale for the WRF and RCA4 models. In contrast, the biases are larger at smaller temporal scale for the CANRCM4 model. Absolute temperatures biases show different patterns for the three RCMs across different temporal scales and periods. Tmin and Tmax simulated by the WRF model are negatively biased with differences of up to -6°C for Tmax, and up to -8°C for Tmin in the JJA period (Figure 4a). Tmax have positive biases in both RCA4 (Figure 4b) and CANRCM4 (Figure 4c) simulations across

Preprints (www.preprints.org) | NOT PEER-REVIEWED | Posted: 25 December 2019 doi:10.20944/preprints201912.0329.v1

Peer-reviewed version available at Water 2020, 12, 364; doi:10.3390/w12020364

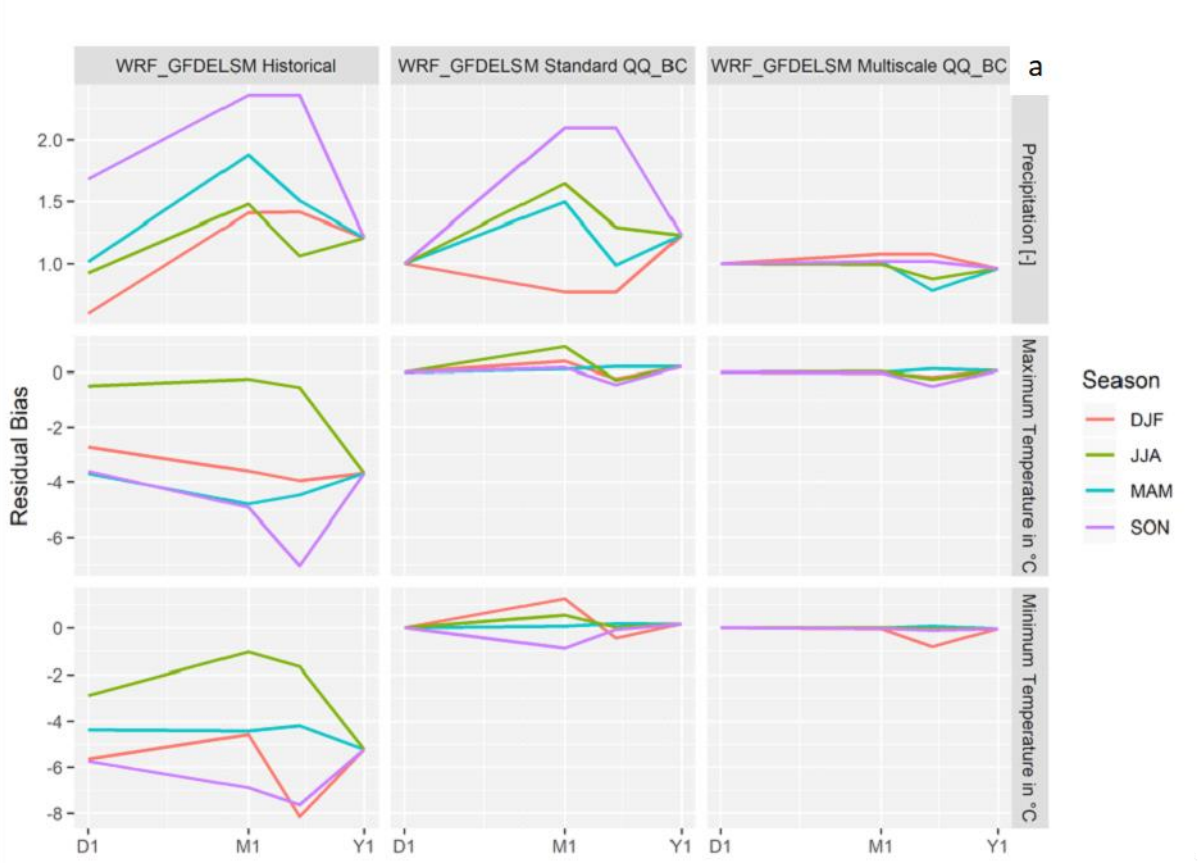

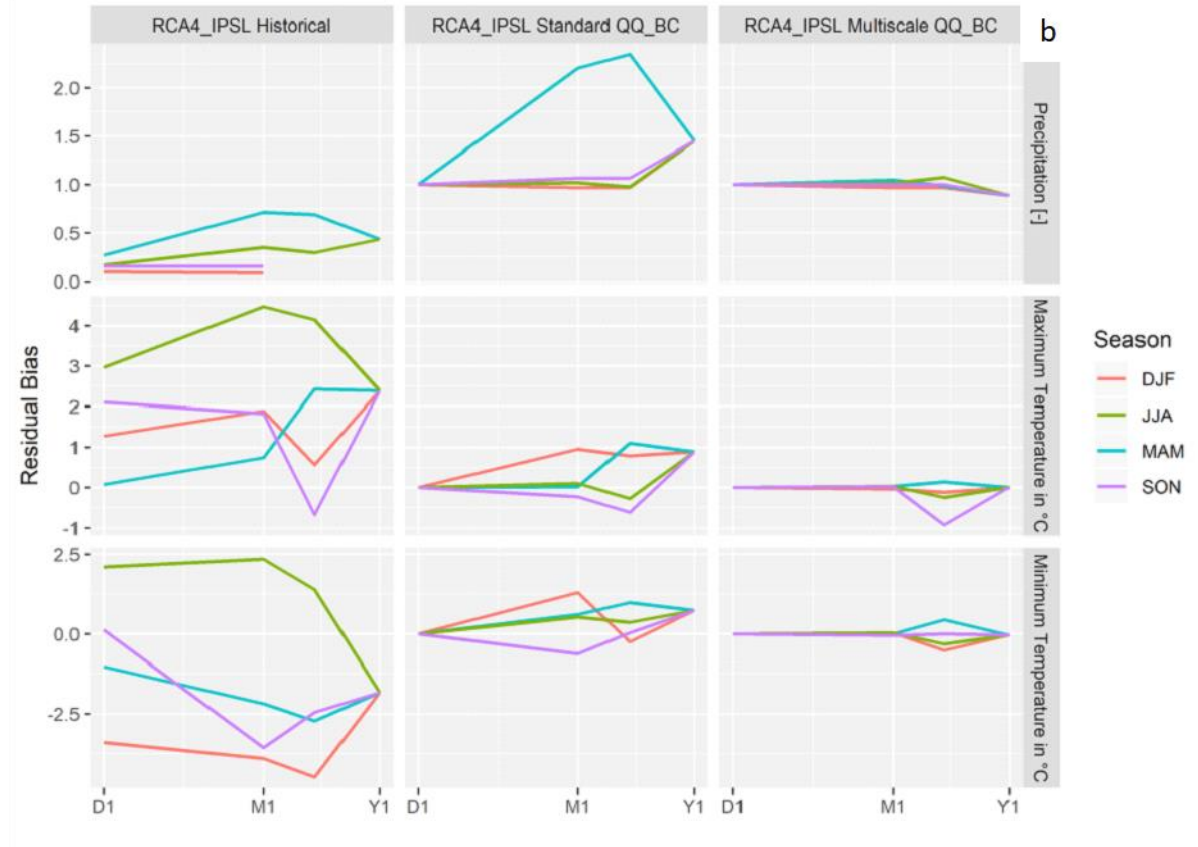

Preprints (www.preprints.org) | NOT PEER-REVIEWED | Posted: 25 December 2019 doi:10.20944/preprints201912.0329.v1

Peer-reviewed version available at Water 2020, 12, 364; doi:10.3390/w12020364

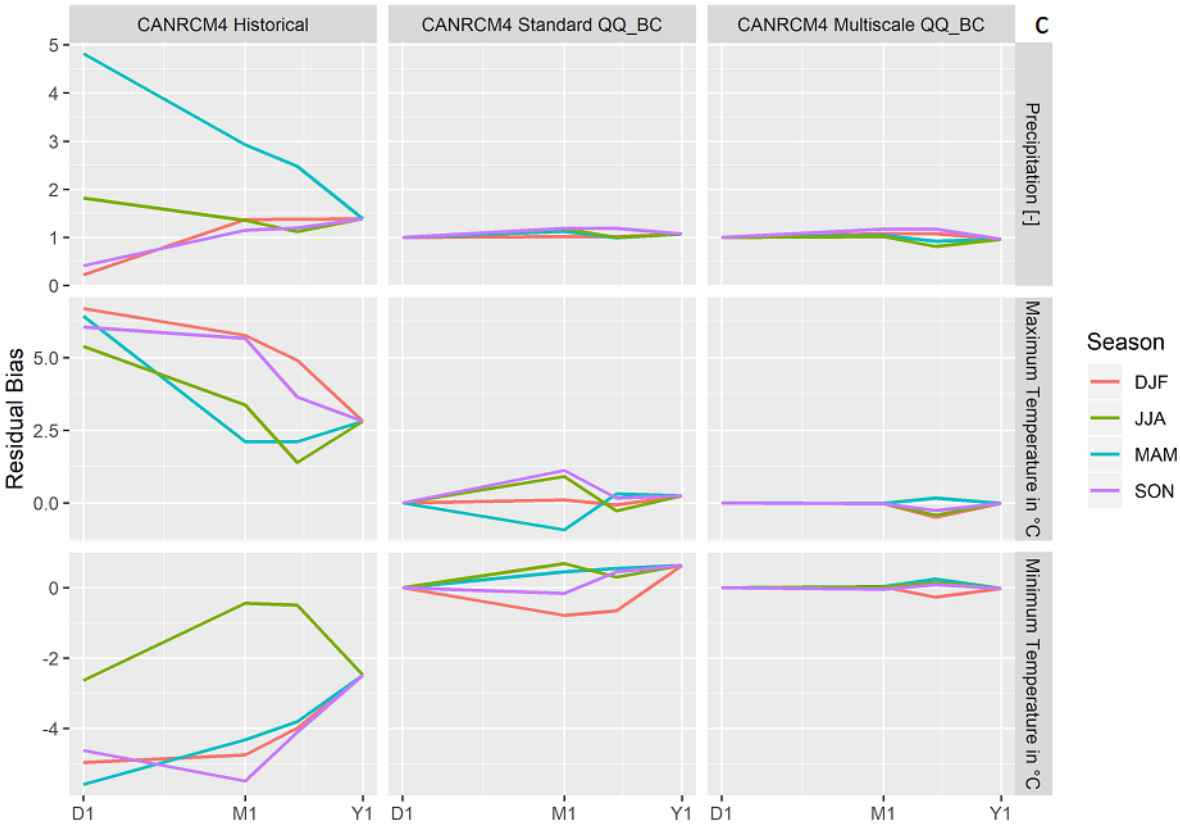

Figure 4. Standard quantile mapping and multiscale bias correction for the three RCMs: (a) WRF; (b) RCA4; (c) CANRCM4.

all periods except for the SON period for the RCA4 model, which has a slight negative Tmax bias. Tmin in the RCA4 and CANRCM are negatively biased across all the periods, except for the JJA period of the RCA4 that has both positive and negative Tmin biases.

The residual rainfall bias across the whole range of temporal scales is significantly reduced (less than 100%) by the standard quantile bias correction methods for all the periods. The multiscale bias correction method produced the same performance for the CANRCM4 model. For a given model, the standard bias correction method was more efficient at the daily timescale, while biases remain large at the monthly timescale (up to 2%). The multiscale bias correction method eliminated the residual temperatures biases across all the timescales for the all periods.

As for WRF and RCA4 models, the standard bias correction reduced slightly rainfall residual bias at daily (D1) and increased the biases at monthly (M1) timescales. The multiscale bias correction method removed significant bias at all the temporal scales. For both models, temperatures biases were completely removed by the multisclae bias correction method at all temporal scales, while in the standard method temperature biases were still important at monthly (M1) timescales. In general, both bias correction methods performed better for temperature than rainfall. The standard quantile mapping method proved to be more efficient at the daily timescale (D1) than at the monthly timescale (M1), while the multiscale method performed well across all temporal scales considered. Therefore, even though the WRF model has a higher spatial resolution (12 km) compared to the CANRCM4 and RCA4 models (50 km), it does not improve the model performance. Statistical downscaling appear to be necessary when using such biased models in impact studies.

3.2 Validation of historical simulations against observed groundwater levels

Preprints (www.preprints.org) | NOT PEER-REVIEWED | Posted: 25 December 2019 doi:10.20944/preprints201912.0329.v1

Peer-reviewed version available at Water 2020, 12, 364; doi:10.3390/w12020364

It was shown in the previous section that even the statistically downscaled historical climate simulation data used to force the hydrological model still have substantial biases; therefore, a validation of historical hydrological simulations is necessary before any impact studies driven by these climate forcing data. The depth to groundwater table and groundwater heads will be used as metrics for the validation of the subsurface component of the HGS model. Depth to groundwater is a variable of great interest for water resources managers in the study area. It is crucial for drilling and managing water supply wells for both drinking and agriculture purposes. The elevation of the depth to groundwater table is calculated in HGS as a linear interpolation of the pressure head at a null pressure level. Depth to groundwater table is then derived from subtraction between the elevation of the groundwater table and surface elevations calculated from the Digital Elevation Model (DEM).

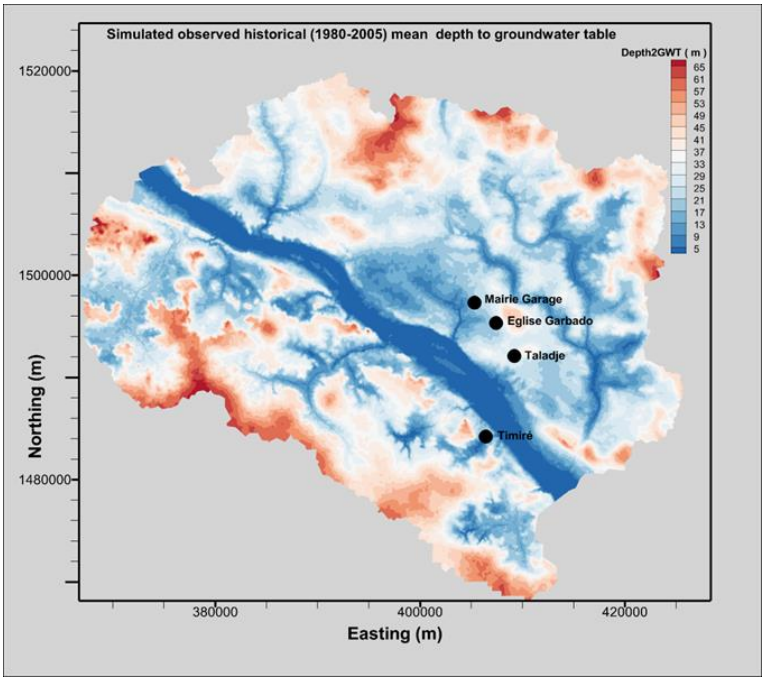

Figure 5. Simulated observed historical mean depth to groundwater table for (1980-2005).

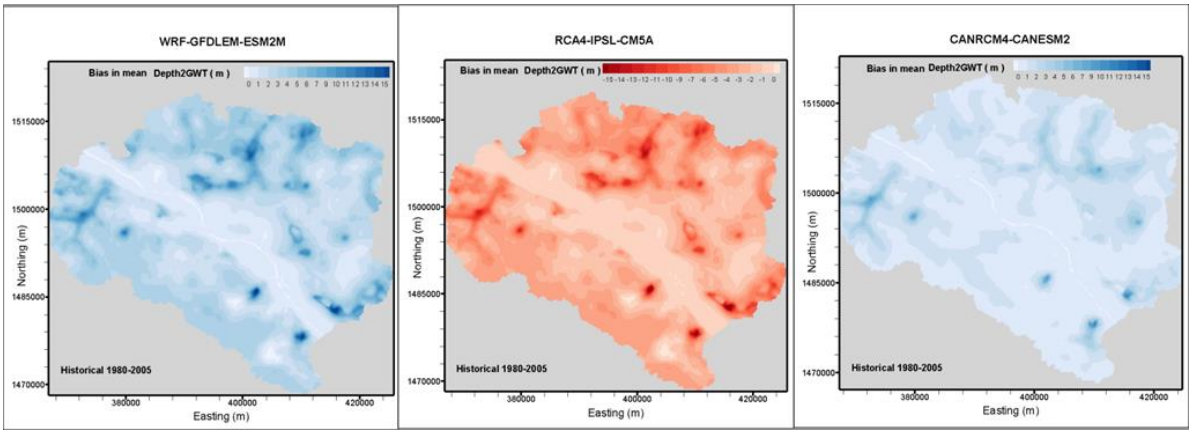

Figure 6. Bias in mean depth to groundwater table.

The observed and simulated depths to groundwater table corresponding to the historical period 1980-2005 are mapped in Figure 5. Four groundwater observation well locations are plotted in Figure 5, and they will be used in the next section to show the long-term simulated groundwater heads transient trend (Figure 6). Across the study area, the average depth to groundwater table ranges from less than 5 m to 65 m (Figure 5). Small depths to groundwater table are generally along the low topographic areas that coincide with either the Niger River or ephemeral streams and ponds where important exchange flux processes between surface water and groundwater occur [37]. Depths to

groundwater table are greater near high land areas and at many piezometric domes as a result of important topographic control on the groundwater flow system in the study area, as shown in previous studies [37,50].

To validate historical simulations of depth to groundwater table for the three RCMs, the bias in mean depth to groundwater table is shown in Figure 6. The bias in mean depth to groundwater table is calculated as difference between simulated observed historical climate data and simulated historical climate scenario for the three RCMs considered.

Simulations with the WRF and CANRCM4 models lead to a higher mean depth to groundwater table, while the RCA4 is negatively biased (Figure 6). Bias in mean depth to groundwater table ranges between 0 to +15 m for WRF and CANRCM4 and between 0 to -15 m for the RCA4. Therefore, simulated historical climate scenarios are drier for the WRF and CANRCM4 models and wetter for the RCA4 model compared to simulated observed historical depth to groundwater table. This should directly be linked to residual bias of rainfall introduced by the multiscale bias correction method (see Figures 4a, 4b and 4c), where RCA4 still have greater positive rainfall bias compared to WRF and CANRCM4 for the JJA (rainy season) period.

The bias in mean depth to groundwater table is spatially different in the study area with high topographic areas having more bias than lower zones. The effect of topography on the bias will be discussed thoroughly in the section 4. However, it is still important to validate simulations against the long-term transient groundwater heads to better analyze how historical climate scenario perform in reproducing long-term seasonal groundwater heads variations. Time series of simulated groundwater heads at four observation wells (see Figure 5 for locations) are shown in Figure 7. Table 2 provides information on wells altitude and distances between wells as well as simulated observed historical and simulated climate scenario heads. The four observation wells were chosen because they have relatively no groundwater pumping and show the important topographical perturbation on groundwater response to climate change. They also have some historical groundwater point heads measurement records.

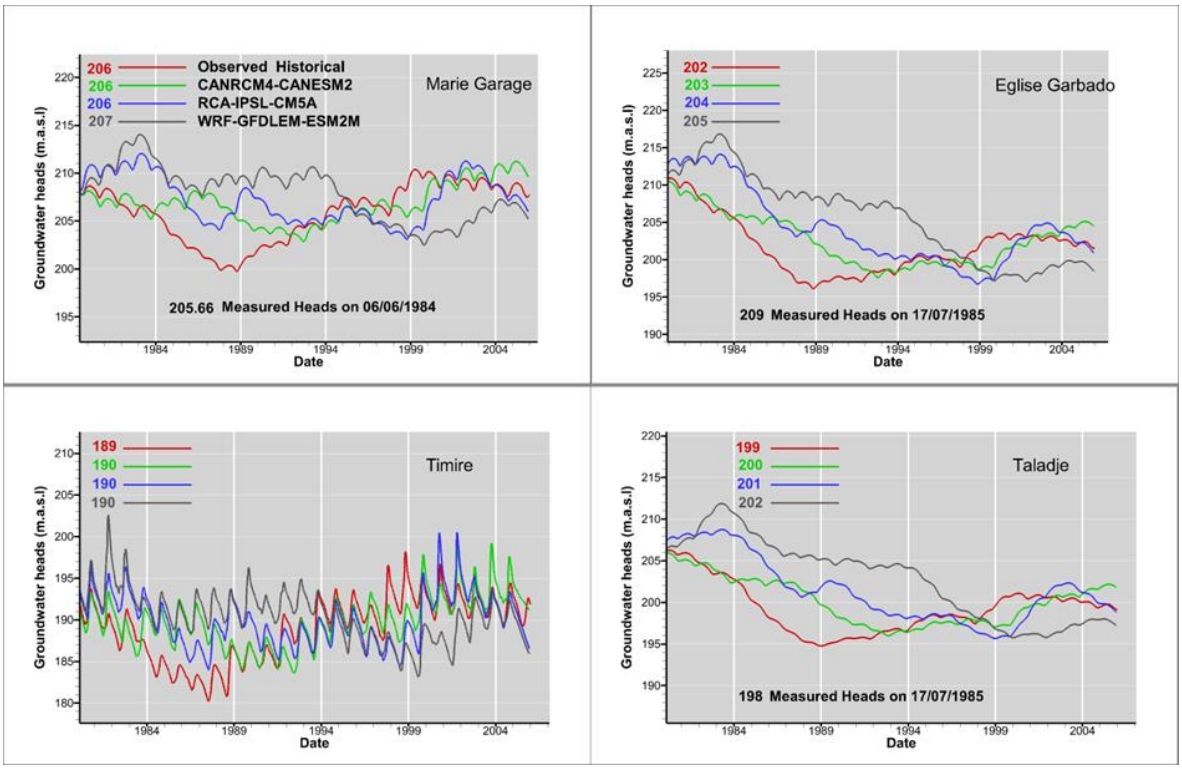

Figure 7. Simulated historical long-term (1980-2005) groundwater heads.

Figure 7 shows that the historical simulated groundwater heads from the climate scenario match reasonably well with the long-term seasonal variability of the observed simulated historical

groundwater heads. Average (1980-2005) groundwater heads are shown as values, and groundwater heads measurements are plotted at the bottom of each figure. Theses measured groundwater heads were reconstituted from historical measurements performed during the 1980s at the construction of the boreholes (Figure 7). All three RCMs tend to overestimate the groundwater heads for 1980-1994 and underestimate heads for 1994-2005. WRF shows the largest dry (wet) groundwater heads bias, and CANRCM4 has the smaller dry (wet) heads bias, while the CRA4 lies in between them (Figure 7). Historical transient groundwater heads as simulated herein show a general decrease between 1980-1994 and an increase from 1994-2005. This long-term increase of groundwater heads is probably due to the recent Sahelian rainfall regime changes recorded in the central part of the Sahel [51], where the 1989-2007 average rainfall exceeded by 10% the average rainfall for 1979-1990. The increase in groundwater heads highlights the important sensitivity of the groundwater response to rainfall pattern changes.

Table 2. Groundwater observation wells with the aquifer types, altitudes, distances between wells, and groundwater heads for the three RCMs.

Well Name	Aquifer Type	Altitude	Simulated Observed Historical Heads	Distance (km)	CANRCM4	RCA4	WRF
Mairie Garage	Fractured Granites	220.6	206.0		206.7	206.8	207.4
Eglise Garbado	Fractured Schistes	221.7	201.8	3.2	202.7	203.8	205.0
Taladje	Fractured Quartzite	225.0	199.4	3.5	200.1	201.1	202.3
Timire	CT3	210.0	189.2	7.0	189.7	189.5	189.9

Table 2 shows the mean absolute errors between simulated observed historical and climate scenario groundwater heads. The mean error seems to be greater at observation wells where depth to groundwater table is deep and smaller at shallow groundwater table. This topographic perturbation of groundwater response to climate change was recently shown by [22] in the Grand River watershed, Canada. For [22], the topographic perturbation is not important within a few km in horizontal resolution. However, Table 2 shows that in the study area, the topographic perturbation is still important even for wells located within shorter distances. As soon as the altitude gradient exists, wells at high topographic positions are more biased than wells located in topographically low areas.

3.3 Validation of historical simulations against surface flowrate

Measured surface flowrates of the Niger River at the Niamey gauging station are used to validate the surface component of the integrated HGS model. Figure 8 shows the measured and simulated historical flowrates for 1980-2005. Simulated flowrates match the measured flow well during all the simulated periods.

Preprints (www.preprints.org) | NOT PEER-REVIEWED | Posted: 25 December 2019 doi:10.20944/preprints201912.0329.v1

Peer-reviewed version available at Water 2020, 12, 364; doi:10.3390/w12020364

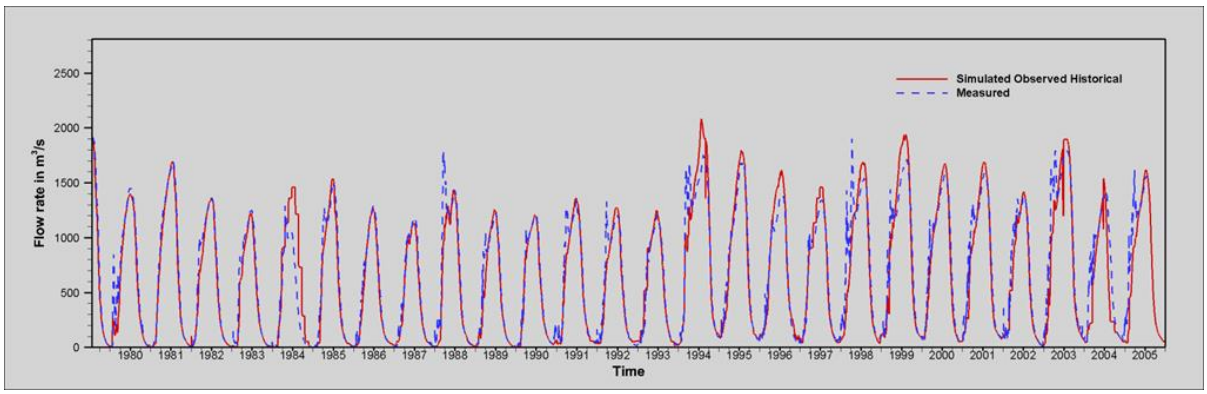

Figure 8. Validation of simulated historical surface water flowrates against measurements.

3.4. Projected changes in local climate

The projected climate change scenarios are presented as relative differences for rainfall (Figure 9a) and as absolute differences for mean temperature (Figure 9b) between simulated historical and mid-century periods. All three RCMs consistently projected an increase in the mean annual rainfall with the CANRCM4 model projecting a mean annual increase of 1.66% followed by the WRF model projecting a rainfall increase of 1.35% and the RCA4 model with an increase of 1.05%. During the rainy season (JJA), WRF and CANRCM4 models project a large increase in rainfall, while the RCA4 project a drier future (Figures 9a and 9b). Similar to rainfall, mean annual temperatures are projected to increase by +1.58°C for RCA4, 1.57°C for CANRCM4, and 1.09°C for WRF. For all three models, greater temperature increases are projected for the MAM period, while increases are relatively smaller for the JJA and SON periods.

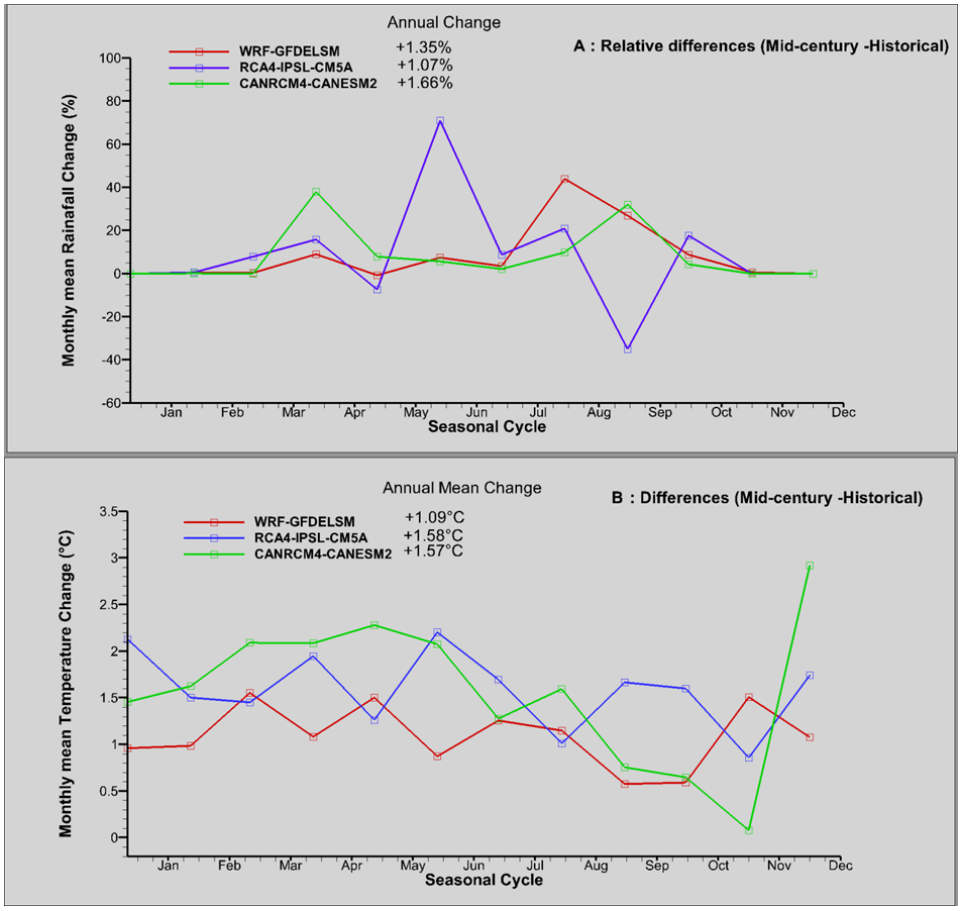

Figure 9. Rainfall and temperatures changes between 2020-2050 (mid-century) and 1980-2005 (historical) at Niamey Airport Station.

3.5. Changes in minimum environmental flow

As previously stated, the Niger River is the only permanent surface water feature from which water is continuously pumped to provide drinking and irrigation water for Niame. Therefore, even though guidance on projected climate change impacts on river discharge is useful information, in this study, minimum environmental flow is used as the climate change impact on surface water. The Minimum Environmental Flow (MEF) is defined as the minimum flowrate of the Niger River at Niamey required to satisfy the drinking and agriculture water demand. Herein, the required minimum low flow value considered for Niamey is 55 m^3/s for 10 days average period, as defined in the 2005 reference period [52]. To assess occurrence and duration of the MEF by the end of the mid-century period (2020-2050), a python command line tool (free at GitHub https://github.com/aerler) was developed that takes as input a HGS hydrograph file, resamples it to daily average values, and counts the occurrence and duration of low/high flow.

MEF duration and occurrences are assessed under historical runoff (1980-2005), where the mid-century runoffs are kept to the historical levels (Figure 10a), and under 10% runoff reduction scenarios (Figure 10b), where runoff conditions are considered to be reduced by 10% compared to historical levels. Overall, all three model almost agree for the occurrence of the MEF with different durations ranging from 10 to 120 days under both historical and -10% runoff scenarios.

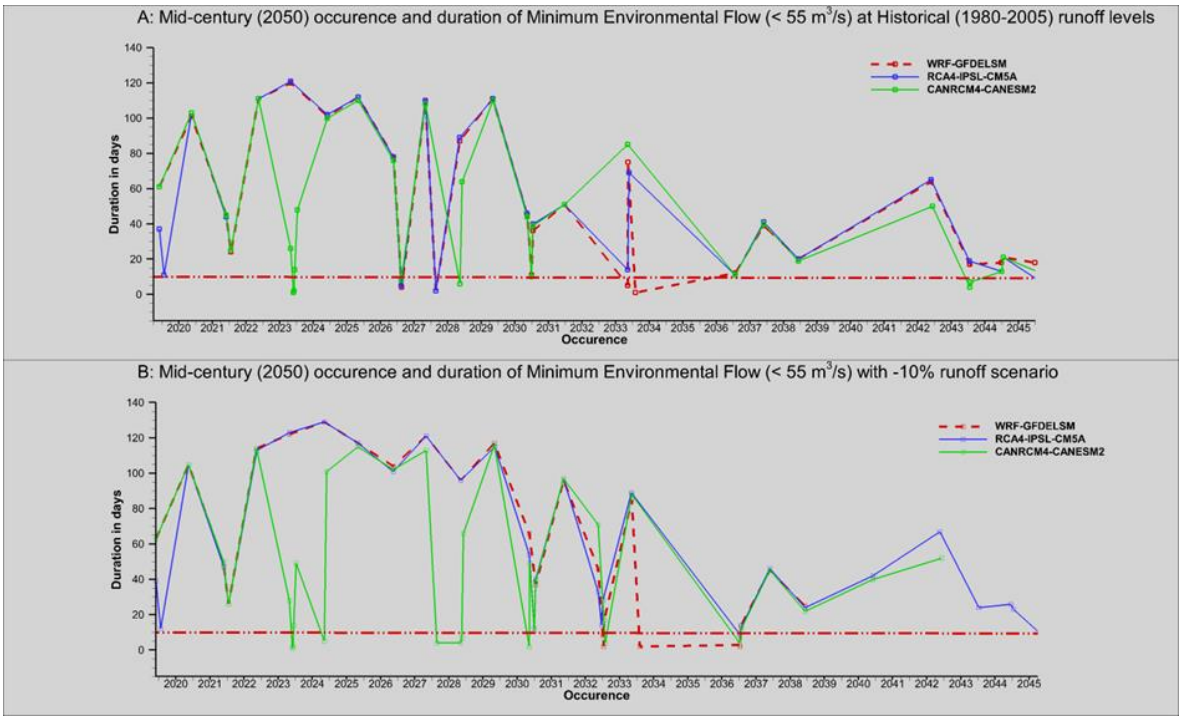

Figure 10. Projected occurrence and duration of Minimum Environmental Flow (MEF) at Niamey gauging station: (a) runoff kept at historical level scenario, and (b) scenario of -10% runoff change compared to historical level.

For the historical runoff level scenario, all three climate models agree on the MEF occurrences for the critical duration level (shown as straight red line in Figures 10a and 10b), defined as a period of 10 consecutive days when the minimum flow required to satisfy drinking and irrigation water demand is not meet. MEF will not be satisfied once every year from 2020 to 2025 and three times every five years between 2025 and 2035; then, occurrences will decrease to once every five years from 2035 to 2050 (Figure 10a). Obviously, conditions of MEF will be severe for the first decade (2020-2030) of the mid-century, and they will become more favorable for the last two decades of the mid-century period. This is mostly due to the dry historical period of 1980-1990 that the Niger River has experienced.

Table 3. Duration of the Minimum Environmental Flow (MEF) under historical and -10% runoff scenarios.

Historical Runoff Scenario	Mid-century (2020-2049) MEF Durations (days)	
	2020-2030 Period	2030-2045 Period
CANRCM4	53	30
RCA4	70	31
WRF	76	28
-10% Runoff Reduction Scenario	Mid-century (2020-2049) MEF average Durations (days)	
	2020-2030 Period	2030-2045 Period
CANRCM4	54	33
RCA4	88	32
WRF	96	32

For the scenario of -10% runoff reduction compared to historical, the occurrences of the MEF are almost the same as for the historical levels with different durations. Durations of MEF are shown in Table 3 for both scenarios. Average durations of the MEF ranges from 53 to 76 days for 2020-2030 and between 28 to 31 days for 2020-2045 under the historical runoff scenario (Table 3). MEF average durations increase under the -10% flow reduction scenario with durations ranging from 54 to 96 days for 2020-2030 and between 32 to 33 days for 2030-2045.

Table 3 and Figures 10a and 10b have shown that durations of the MEF are sensitive to runoff reduction with projected patterns of MEF directly influenced by the changes in net precipitation of the climate scenario models. Dry (wet) models predict recurrent (less frequent) and high (low) MEF conditions by the end of mid-century. MEF conditions were previously shown to also be sensitive to runoff reduction for two gauging station located upstream of the study area [52].

3.6. Changes in depth to groundwater table

Figure 11 (top panel) shows the projected mean changes of depth to groundwater table (Depth2GWT) for the three RCMs. All three RCMs show an increase of groundwater table ranging from +2 m to more than +15 m. The CANRCM4 model predicts the greater increase of groundwater table followed by the WRF and RCA4 models. The groundwater table is likely to increase more in high topographic areas, where depth to groundwater table is deep, than topographic low areas with relatively shallow depth to groundwater table. For CANRCM4 and WRF models, mean groundwater table increased by an average of 4 m in low altitude area and by more than 12 m in topographic areas. While the RCA4 model predicts a maximum increase of +1 m in shallow groundwater table area and an increase of 3 m in deep groundwater table area (Figure 11). Therefore, as seen for the MEF change patterns, groundwater table response to climate change is strongly dictated by the climate change forcing signal, particularly in mean annual net precipitation changes.

The groundwater table response to climate change is more perturbed in topographically high areas than in low altitude zones (Figure 11). To illustrate the topographical effect on groundwater table response to climate change, cross section was drawn along NE-SW of the study area (Figure 11, bottom). Changes in depth to groundwater table for the CANRCM4 model are shown in the colored contour, and groundwater heads are represented as line contours. It is obvious that greater changes in depth to groundwater table are located in areas where the groundwater heads are also greater. The topographic perturbation is still evident even within small horizontal distances (2 km). This may be explained by the intensity of seasonal variation of groundwater table with less variation in low topographic areas that are groundwater discharge areas in which exhange flux mostly occurs with surface water. However, high altitude areas are generally direct groundwater recharge areas.

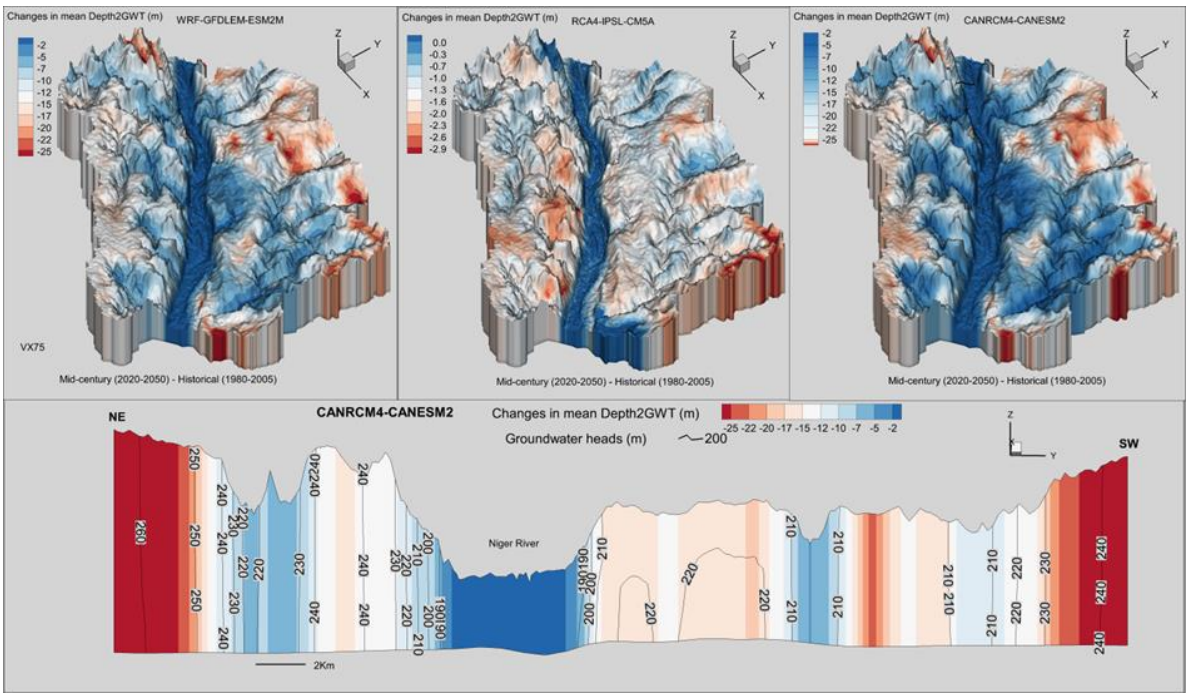

Figure 11. Changes in depth to groundwater table: top panel shows mean changes in depth to groundwater table by the mid-century for the three RCMs; bottom panel shows a 2D cross-section for the CANRCM.

Erler et al. [22] have shown that the topographical perturbation of groundwater table in response to climate change is only important in large scale topographic gradients. However, the climate induced topographical perturbation of groundwater table in response to climate change is important even in small-scale topographic gradients as shown in Figure 11. This difference is probably due to different climate conditions, as herein, intense monsoonal rainfall induces a large seasonal groundwater table variation, while in Grand River Watershed, the precipitation is evenly distributed throughout the year [22]. Also, local topography has a more pronounced control in the groundwater flow system in the study area [37,50] than in the Grand River Watershed.

3.7. Implications of changes in adaptation strategies

Based on the projections made on surface water response to climate change impacts, Niamey watershed in general, and the city in particular, will experience recurrent and long periods where the MEF conditions will be under the required level. The risk level is even increased when the -10% runoff scenario is considered. However, the mid-century climate projections signal is wetter for all three RCMs used, which means that historical runoff level reduction is less probable. An increase in the irrigation water demand during the dry period in the upstream of Niamey will probably create a high surface water stress risk if the ongoing Kandadji dam construction that is supposed to maintain the MEF is not completed.

On the other hand, basin wide groundwater table rise is projected with greater increase at deep water table and relatively smaller increase at shallow water table depth. Therefore, considering the current population and urbanization rates, groundwater represents a sustainable adaptation pathway for the recurrent water stress that will be induced by the high sensitivity of the Niger River MEF to climate change impacts.

4. Summary and conclusions

The integrated hydrological response to climate change impact has been assessed on a large-scale, semi-arid watershed using the fully integrated HGS model. The model was calibrated sequentially for long-term steady state (1980-2005), dynamic equilibrium, and fully transient conditions. Three RCMs models were bias corrected at daily, monthly, and yearly timescales.

Performance of the HGS simulations forced by the three bias corrected RCMs was then evaluated against simulations forced by observed historical HGS simulations using both surface water flowrate and depth to groundwater table as metrics. Mid-century (2020-2050) climate change scenario simulations were performed with the three RCMs, and MEF and groundwater table responses were evaluated under historical runoff and -10% runoff scenarios.

Bias correction of the historical climate scenario shows that the quantile mapping correction performed better at daily and yearly timescales than at monthly timescales. Simulations of historical depth to groundwater table by the three RCMs is positively biased compared to observed historical climate simulations with large biases at higher groundwater table depth. The resolution of the forcing RCM was found to not improve significantly its performance. All RCMs project an increase in mean annual rainfall and in mean annual temperatures. The signals of mid-century rainfall changes are directly translated into the depth to groundwater table response to climate change with a general groundwater table increase predicted by the three RCMs. MEF durations show a high sensitivity to runoff reduction. The groundwater table is also found to increase more at higher altitude than at low altitude areas.

Fully physics-based integrated hydrological models have been shown to represent one of the most reliable ways to assess climate change impacts on groundwater [20,22,53,54]. However, the application of theses integrated models is computationally expensive, resulting in few published applications of integrated hydrological models at large scale [53]. Large-scale anthropogenic climate change impacts using integrated hydrological models are rarely investigated in the scientific literature. To the authors' knowledge, there are only three published climate change impact studies that employed fully integrated models [22-24]. However, in all these studies, either small scales or relatively coarse meshed resolution were used [23,24], or simulations were performed using representative seasonal cycles to reduce the computational cost [22]. Also, previously cited assessments were all performed in wet climate conditions, in more developed countries, and where sufficient data are more available. Therefore, the novelty of this study is that simulations with higher resolution (up to 70 m) at large scale (1,900 Km^2) were performed in semi-arid climate environments with sparse data. While acknowledging the data challenge for model validations, the use of higher mesh resolution seems to improve simulation quality and to some extent compensate for the sparse data issue.

Development and application of fully integrated hydrological models can provide reliable guidance in addressing concern about the combined response of surface water and groundwater to future climate change impacts. It is, therefore, possible even with modest computing resources and sparse data to provide to water resource managers in developing countries decision-making tools to define integrated climate change adaption strategies.

Funding: This research was funded by the German Federal Ministry of Education and Research (BMBF), grant number 01LG1202E of the WASCAL project, and Aquanty's Visiting Student Program.

Conflicts of Interest: The authors declare no conflict of interest.

References

1. Niger PRSP. Accelerated development and poverty reduction strategy, 2008–2012. In *Combating Poverty, A Challenge for All*; International Monetary Fund: Niamey, Niger, 2008.
2. INS. *Statistical Demographic Yearbook*; National Institute of Statistics Niger: Niamey, Niger, 2012.
3. United Nations Framework Convention on Climate Change (UNFCC 2009): Climate Change - Impacts, Vulnerabilities and Adaptation in Developing Countries. Available online: www.unfccc.int (accessed 2009).
4. Kundzewicz, Z.W.; Mata, L.J.; Arnell, N.; Döll, P.; Kabat, P.; Jiménez, B.; Miller, K.; Oki, T.; Şen, Z.; Shiklomanov, I. Freshwater resources and their management. In *Climate Change 2007: Impacts, Adaptation and Vulnerability. Contribution of Working Group II to the Fourth Assessment Report of the Intergovernmental Panel on Climate Change*; Parry, M.L., Canziani, O.F., Palutikof, J.P., van der Linden, P.J., Hanson, C.E., Eds.; Cambridge University Press: UK, 2007; pp. 173-210.

5. Kundzewicz, Z.W.; Krysanov, V.; Benestad, R.E; Hov, Ø; Piniewski, M,; Otto, I.M. Uncertainty in climate change impacts on water resources. *Env. Sci. and Policy* **2018**, 79, 1-8.
6. Shen, M.; Chen, J.; Zhuan, M.; Chen, H.; Xu, C-Y; Xiong, L. Estimating uncertainty and its temporal variation related to global climate models in quantifying climate change impacts on hydrology. *J. Hydrol.* **2018**, 556, 10-24.
7. Clark, P.M.; Wilby, L.R.; Gutmann, D.E.; Vano, A.J.; Gangopadhyay, S.; Wood, W.A.; Fowler, J.H.; Prudhomme, C.; Arnold, R.J.; Brekke, D.L. Characterizing uncertainty of the hydrologic impacts of climate change. *Current Climate Change Report* **2016**, 2, 55-64.
8. Goderniaux, P.; Brouyère, S.; Wildemeersch, S.; Therrien, R.; Dassargues, A. Uncertainty of climate change impact on groundwater reserves - Application to a chalk aquifer. *J. Hydrol.* **2015**, 528, 108-121.
9. Refsgaard, J.C.; Sonnenborg, T.O.; Butts, M.B.; Christensen, J.H.; Christensen, S.; Drews, M.; Vilhelmsen, T.N. Climate change impacts on groundwater hydrology - Where are the main uncertainties and can they be reduced? *Hydrol. Sci. J.* **2016**, 61(13), 2312-2324.
10. Moeck, C.; Brunner, P.; Hunkeler, D. The influence of model structure on groundwater recharge rates in climate-change impact studies. *Hydrogeol. J.* **2016**, 24(5), 1171-1184.
11. Kurylyk, B.L.; MacQuarrie, K.T.B. The uncertainty associated with estimating future groundwater recharge: A summary of recent research and an example from a small unconfined aquifer in a northern humid-continental climate. *J. Hydrol.* **2013**, 492, 244-253.
12. Stoll, S.; Hendricks-Franssen, H.J.; Butts, M.; Kinzelbach, W. Analysis of the impact of climate change on groundwater related hydrological fluxes: A multimodel approach including different downscaling methods. *Hydrol. Earth Syst. Sci.* **2011**, 15(1), 21-38.
13. Bastola, S.; Murphy, C.; Sweeney, J. The role of hydrological modelling uncertainties in climate change impact assessments of Irish river catchments. *Adv. Water Resources* **2011**, 34, 562-576.
14. Van Roosmalen, L.; Sonnenborg, T.O.; Jensen, K.H. Impact of climate and land use change on the hydrology of a large-scale agricultural catchment. *Water Resources Res.* **2009**, 45(7), 1-18.
15. Bates, B.C.; Kundzewicz, Z.W.; Wu, S.; Palutikof, J.P. *Climate Change and Water Technical Paper*. Intergovernmental Panel on Climate Change: Geneva, 2008.
16. Taylor, R.G.; Koussis, A.; Tindimugaya, C. Groundwater and climate in Africa: A review. *Hydrol. Sci. J.* **2009**, 54, 655-664.
17. Nkhonjera, G.K.; Dinka, O.M. Significance of direct and indirect impacts of climate change on groundwater resources in the Olifants River basin: A review. *Global Planetary Change* **2017**, 158, 72-82.
18. Armandine Les Landes, A. ; Aquilina, L. ; De Ridder, J. ; Longuevergne, L. ; Pagé, C. ; Goderniaux, P. Investigating the respective impacts of groundwater exploitation and climate change on wetland extension over 150 years. *J. Hydrol.* **2014**, 509, 367-378.
19. Holman, I.; Allen, D.; Cuthbert, M.; Goderniaux, P. Towards best practice for assessing the impacts of climate change on groundwater. *Hydrogeol. J.* **2012**, 20(1), 1-4.
20. Goderniaux, P.; Brouyère, S.; Fowler, H.J.; Blenkinsop, S.; Therrien, R.; Orban, P.; Dassargues, A. Large scale surface-subsurface hydrological model to assess climate change impacts on groundwater reserves. *J. Hydrol.* **2009**, 373(1-2), 122-138.
21. Green, T.R.; Taniguchi, M.; Kooi, H.; Gurdak, J.J.; Allen, D.M.; Hiscock, K.M.; Treidel, H.; Aureli, A. Beneath the surface of global change: Impacts of climate change on groundwater. *J. Hydrol.* **2011**, 405(3-4), 532-560.
22. Erler, A.R; Frey, S.K.; Khader, O.; d'Orgeville, M.; Park, Y.-J.; Hwang, H.-T.; Lapen D.; W.P.R.; Sudicky, E.A. Climate change impacts on groundwater resources based on integrated hydrologic modeling and high-resolution climate projections within a lake-affected region. *Water Resources Res.* **2019**, 55, 8142-8163.
23. Goderniaux, P.; Brouyère, S.; Blenkinsop, S.; Burton, A.; Fowler, H.J.; Orban, P., Dassargues, A. Modeling climate change impacts on groundwater resources using transient stochastic climatic scenarios. *Water Resources Res.* **2011**, 12, 52-16.
24. Sulis, M.; Paniconi, C.; Marrocu, M.; Huard, D.; Chaumont, D. Hydrologic response to multimodel climate output using a physically based model of groundwater/surface water interactions. *Water Resources Res.* **2012**, 48(12), 1-18.
25. MacDonald, A.M.; Bonsor, H.C.; Dochartaigh, B.É.Ó.; Taylor, R.G. Quantitative maps of groundwater resources in Africa. *Environ. Res. Lett.* **2012**, 7(2), 1-7.
26. Toure, A.; Diekkrüger, B.; Mariko, A. Impact of climate change on groundwater resources in the Klela Basin, Southern Mali. *Hydrol*. **2016**, 3(2), 1-17.

27. Nyenje, P.M.; Batelaan, O. Estimating the effects of climate change on groundwater recharge and baseflow in the upper Ssezibwa catchment, Uganda. *Hydrol. Sci. J.* **2009**, 54(4), 713-726.
28. Desconnets, J.C.; Taupin, J.D.; Lebel, T.; Leduc, C. Hydrology of the Hapex-Sahel Central Super-Site: Surface water drainage and aquifer recharge through the pool systems. *J. Hydrol.* **1997**, 188-189, 155-178.
29. Leduc, C.; Bromley, J.; Schroeter, P. Water table fluctuation and recharge in semi-arid climate: Some results of the HAPEX-Sahel hydrodynamic survey (Niger). *J. Hydrol.* **1997**, 188-189, 123-138.
30. Favreau, G. Characterization and modelling of a rising water table in the Sahel: Dynamics and geochemistry of the Dantiandou kori natural piezometric depression (Southwest Niger). Ph.D. Thesis, Univ Paris XI, Orsay, France, 2000.
31. Favreau, G.; Nazoumou, Y.; Leblanc, M.; Guero, A; Goni, I.B. Groundwater resources increase in the Iullemmeden Basin, WestAfrica. In *Climate Change Effects on Groundwater Resources: A Global Synthesis of Findings and Recommendations*; Treidel, H., Martin-Bordes, J.L., Gurdak, J.J., Eds.; International Contributions to Hydrogeology 27, CRC, Leiden, The Netherlands, 2012 ; pp 113-128.
32. Milly, P.C.D.; Dunne, K.A. A hydrologic drying bias in water-resource impact analyses of anthropogenic climate change. *J. Am. Water Resources Assn.* **2017**, 53(4), 822-838.
33. Chen, J.; Sudicky, E.A.; Davison, J.H.; Frey, S.K.; Park, Y.-J.; Hwang, H.-T.; Erler, A.R.; Berg, S.J.; Callaghan, M.V.; Miller, K.; Ross, M.; Peltier, W.R. Towards a climate-driven simulation of coupled surface-subsurface hydrology at the continental scale: A Canadian example. *Can. Water Resources J.* (under review).
34. Soumaïla, A.; Konaté, M. Characterization of the deformations in the Birimian (Palaeoproterozoic) belt of the Diagorou-Darbani (Nigerien Lipatako, West Africa). *Africa Geosci. Rev.* **2005**, 12(3), 161-178.
35. Machens, E. Contribution to the study of the crystalline basement and sedimentary formations of the West Niger Republic region. 3 Mém. BRGM, Fr., 1973, n° 82; 167 pp.
36. Perotti, L.; Dino, A.G.; Lasagna, M.; Konaté, M.; Spadafora, F.; Yadji, G.; Tankari, D.-B. A.; De Luca, A.D. Monitoring of urban growth and its related environmental impacts: Niamey case study (Niger). *Energy Procedia* **2016**, 97, 37-43.
37. Boubacar, A.B.; Moussa, K.; Yalo, N.; Berg, S.J.; Erler, A.R.; Hwang, H.-T.; Khader, O.; Sudicky, E.A. Characterization of groundwater-surface water interactions using high resolution integrated 3D hydrological model in semiarid urban watershed of Niamey, Niger. *J. African Earth Sci.* (under review).
38. Bigi, V.; Pezzoli, A.; Maurizio, R. Past and future precipitation trend analysis for the City of Niamey (Niger): An overview. *Climate* **2018**, 6, 73-89.
39. Ramier, D.; Boulain, N.; Cappelaere, B.; Timouk, F.; Rabanit, M.; Lloyd, C.R.; Boubkraoui, S.; Metayer, F.; Descroix, L.; Wawrzyniak, V. Towards an understanding of coupled physical and biological processes in the cultivated Sahel: 1. energy and water. *J. Hydrol.* **2009**, 375, 204-216.
40. Aquanty Inc. HGS User Manual. Available online: https://static1.squarespace.com/static/54611cc8e4b0f88a2c1abc57/t/59cea33846c3c4384b8e5de1/1506714438873/hydrosphere_user.pdf (accessed 2018).
41. Hwang, H.T.; Park, Y.-J.; Sudicky, E.A.; Forsyth, P.A. A parallel computational framework to solve flow and transport in integrated surface–subsurface hydrologic systems. *Envir. Model Software* **2014**, 61(0), 39-58.
42. Hagemann, S.; Chen, C.; Clark, D.; Folwell, S.; Gosling, S.N.; Haddeland, I.; Hannasaki, N.; Heinke, J.; Ludwig, F.; Voss, F.; Wiltshire, A. Climate change impact on available water resources obtained using multiple global climate and hydrology models. *Earth Syst. Dyn.* **2013**, 4, 129-144.
43. Kristensen, K.J.; Jensen, S.E. A model for estimating actual evapotranspiration from potential evapotranspiration. *Nordic Hydrol.* **1975**, 6, 170-188.
44. Hwang, H.-T.; Park, Y.-J.; Frey, S.K.; Berg, S.J.; Sudicky, E.A. A simple iterative method for estimating evapotranspiration with integrated surface/subsurface flow models, *J. Hydrol.* **2015**, 531(3), 949-959.
45. Hwang, H.-T.; Park, Y.-J.; Sudicky, E.A.; Berg, S.J.; McLaughlin, R.; Jones, J.P. Understanding the water balance paradox in the Athabasca River Basin, Canada. *Hydrol. Processes* **2018**, 32(6), 729-746.
46. Droogers, P.; Richard, A.G. Estimating reference evapotranspiration under inaccurate data conditions. *Irrigation and Drainage Sys.* **2002**, 16, 33-45.
47. Heinzeller, D.; Dieng, D.; Smiatek, G.; Olusegun, C.; Klein, C.; Hamann, I.; Salack, S.; Bliefernicht, J.; Kunstmann, H. The WASCAL high-resolution regional climate simulation ensemble for West Africa: concept, dissemination and assessment. *Earth Syst. Sci. Data* **2018**, 10, 815-835.

48. Mascaro, G.; White, D.D.; Westerhoff, P.; Bliss, N. Performance of the CORDEX-Africa regional climate simulations in representing the hydrological cycle of the Niger River basin. *J. Geophys. Res. Atmos.* **2015**, 120, 12,425-12,444.
49. Hanel, M.; Kozín, R.; Hermanovský, M.; Roub, R. An R package for assessment of statistical downscaling methods for hydrological climate change impact studies. *Envir. Modeling Software* **2017**, 95, 22-28.
50. Hassane, A.B.; Christian, L.; Favreau, G.; Barbara, A.B.; Thomas, M. Impacts of a large Sahelian city on groundwater hydrodynamics and quality: example of Niamey (Niger). *Hydrogeol. J.* **2016**, 24, 407-423.
51. Lebel, T; Ali, A. Recent trends in the Central and Western Sahel rainfall regime (1990-2007). *J. Hydrol.* **2009**, 375, 52-64.
52. Grijsen J.G.; Tarhule, A.; Brown, C.; Ghile, Y.B.; Taner, Ü.; Talbi- Jordan, A.; Doffou, H.N.; Guero, A.; Dessouassi, R.Y.; Kone, S.; Coulibaly, B.; Harshadeep, N. Climate Risk Assessment for Water Resources Development in the Niger River Basin Part II: Runoff Elasticity and Probabilistic Analysis. In *Climate Variability - Regional and Thematic Patterns*; Aondover Tarhule, IntechOpen, 2013; pp. 57-72.
53. Barthel, R.; Banzhaf, S. Groundwater and surface water interaction at the regional-scale: A review with focus on regional integrated models. *Water Resources Mngmt.* **2016**, 30(1), 1-32.
54. Kollet, S.; Sulis, M.; Maxwell, R.M.; Paniconi, C.; Putti, M.; Bertoldi, G.; Coon, E.T.; Cordano, E.; Endrizzi, S.; Kikinzon, E.; Mouche, E.; Mügler, C.; Park, Y.-J.; Refsgaard, J.C.; Stisen, S.; Sudicky, E. The integrated hydrologic model intercomparison project, IH-MIP2: A second set of benchmark results to diagnose integrated hydrology and feedbacks. *Water Resources Res.* **2017**, *53*(1), 867-890.